

CFD simulation and implementation of a griddle-type biomass stove for rural communities

Y. Galindo, D. Gómez-Heleria, J. Núñez*, and C. A. García

Escuela Nacional de Estudios Superiores, Unidad Morelia, Universidad Nacional Autónoma de México, Antigua Carretera a Pátzcuaro No. 8701, Col. Ex Hacienda de San José de la Huerta, 58190, Morelia, Michoacán, México.

Received 23 April 2024; accepted 14 August 2024

This work focuses on the design of a new griddle-type biomass stove with an internal cross-flow configuration. For this purpose, numerical simulations of the heat transfer and fluid flow in the stove have been carried out. In particular, the equations corresponding to the momentum, energy, and chemical species are solved to determine the influence of the geometrical design. Temperature and isothermal contours on the surface of the griddle were presented. Various stove designs with firepower settings ranging from 7 to 16 kW were investigated. The findings revealed a decrease in thermal efficiency with increasing firepower, which was attributed to higher convective losses. Based on the numerical results, a cookstove prototype was manufactured. Furthermore, the thermal efficiency of the stove was evaluated using the WBT protocol. The goal of this research is not only to assess the thermal performance of the developed technology but also to provide a real-world example of the adoption process of a technology designed for rural communities.

Keywords: Computational fluid dynamics; biomass stove; diffusion of technology.

DOI: <https://doi.org/10.31349/RevMexFis.71.010602>

1. Introduction

Biomass cookstoves (BC) are traditional devices used for cooking tasks, mainly in rural areas [1,2]. Many researchers have been interested in employing computational fluid dynamics (CFD) as a tool for optimizing BC [3]. Numerical simulations play an important role in determining the fluid flow, heat transfer, and combustion processes within the cookstove. This is critical for minimizing fuel consumption, reducing emissions, selecting appropriate materials, and testing different designs without having to build physical prototypes.

Numerous methodologies have been proposed for the development of a BC. As is revealed in the literature review, primary research includes laboratory testing of emissions, thermal efficiency evaluation based on the water boiling test (WBT) [4], field testing and survey evaluation [5], as well as social strategies for increasing the adoption of this type of technology [6].

In many cases, reducing emissions from BC is the more important goal in diffusion programs; therefore, combustion and pollutant formation processes are commonly evaluated experimentally [7]. Experimental work as well as a simplified chemical kinetic model suggests that a chimney plays an active role in the performance of a stove by influencing the overall air-to-fuel ratio and subsequently the production of carbon monoxide [8].

The air excess ratio significantly improves the combustion efficiency of a biomass stove and reduces the emissions of particulate matter (PM) [9]. An Experimental Study of Secondary Air Injection in a Wood-Burning Cookstove was presented by Caubel *et al.* [10]. The results show that PM

emissions are highly sensitive to secondary air injection flow rate and velocity.

The combined use of advanced, high-fidelity models and experimental techniques can enable the validation of numerical wood combustion models, reducing the time required for development and providing cleaner and more efficient BC. While computational power requirements will increase [11]; a direct link of the wood log model and the CFD routines, with an exchange of boundary conditions between the time steps of the simulations, is needed in order to save computing time [12]. Commonly, the commercial software ANSYS FLUENT is applied to model the problem, but transient CFD simulations of BC can be performed using free software [13]. The OpenFOAM software is capable of simulating the non-premixed combustion of air and volatiles within the internal volume.

Biomass cookstoves have generally been created through trial and error [14], but CFD simulations are rapidly helping to explore new functionalities, combining biomass with other energy sources [15], or developing new prototypes for specific cooking applications [16]. There must be a balance between technical and user objectives. However, a usability focused design has the potential to achieve higher adoption rates compared to a technologically focused design [17].

CFD analysis was used to investigate the impact of design modifications on the thermal and emissions performance of a natural draft rocket cookstove by Dalbehera *et al.* [18]. Their design modification incorporates a baffle plate of varying dimensions and positions and a multi-directional fuel inlet. The results indicate that the baffle plate promotes turbulent mixing, which facilitates the mixing of combustible gases with air and subsequently improves combustion quality. However,

the size and position of the baffle plate play a significant role in its effectiveness.

Motyl *et al.* [19] conducted a new design for wood stoves based on numerical analysis and experimental research. In the first part, a numerical model is proposed of the fireplace insert including fluid flow, the chemical combustion reaction, and heat exchange. The results of the simulation were compared with the experiment carried out on the test bench. A comparison of the experimental and numerical results was made for the temperature distribution along with the concentration of CO, CO₂, and O₂. Construction changes were proposed in the second stage, together with numerical simulations whose goal was an increase in the efficiency of the heating devices.

Generally, the works reported in the literature develop a stove and then evaluate its performance with a CFD. Thus, few reported cases have reached a level where CFD can be used as a tool for stove design. This work contributes to the development of a biomass cookstove design using CFD that takes into account a parametric analysis of an interior volume to determine which geometry achieves the best performance. The study incorporated user feedback to adjust design features, ensuring practical relevance and usability.

2. Conceptual model

Plancha-type stoves have three main components: a combustion chamber, a chimney, and a mild steel plate (griddle). The internal volume of the biomass stove was used as the computational domain, as shown in Fig. 1. The internal volume defines the domain within which fluid flow behavior is simulated.

The combustion chamber in this configuration is trapezoidal in shape to concentrate the wood in the center. The stove is designed with a cross-flow configuration to increase

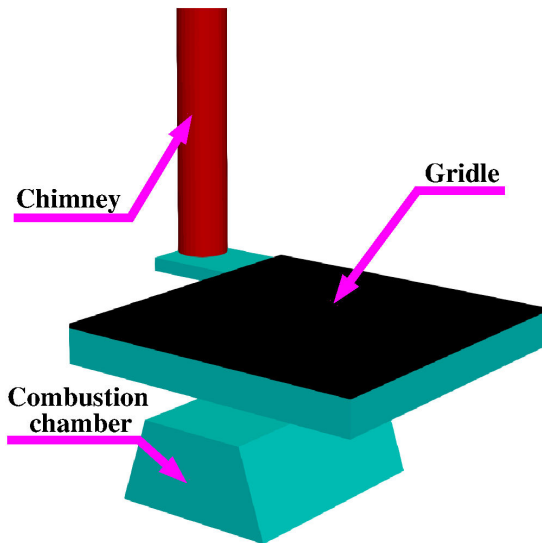


FIGURE 1. First conceptual model with the main parts of a biomass stove.

the distance traveled by the combustion gases, resulting in a larger coverage area.

Traditionally, a “top-down” approach has been used in manufacturing stoves. A “bottom-up” approach is explored since this process starts by evaluating the performance of the inner volume before using it to fabricate a stove. This methodology is aimed at improving process efficiency and product quality. Note that any other interior volume configuration can be studied and used in order to develop a prototype.

2.1. Governing equations

The evaluation of the performance of the stove is based on the equations of conservation of mass, momentum, and energy. For combustion modeling, additional equations are introduced to account for species transport and reaction rates (see [20,21]). A general overview and a list of the key equations for each aspect are provided.

Conservation of mass

$$\frac{\partial \rho}{\partial t} + \nabla \cdot (\rho \vec{v}) = 0, \quad (1)$$

where ρ is the density and \vec{v} the fluid velocity.

Conservation of momentum

$$\frac{\partial}{\partial t}(\rho \vec{v}) + \nabla \cdot (\rho \vec{v} \vec{v}) = -\nabla p + \nabla \cdot (\bar{\tau}) + \rho \vec{g} + \vec{F}, \quad (2)$$

where p is the static pressure, $\bar{\tau}$ is the stress tensor (described below), and $\rho \vec{g}$ and \vec{F} are the gravitational body force and external body forces such user-defined sources.

For Newtonian fluids, the viscous stress tensor $\bar{\tau}$ can be represented as

$$\bar{\tau} = \mu \left[(\nabla \vec{v} + \nabla \vec{v}^T) - \frac{2}{3} \nabla \cdot \vec{v} I \right], \quad (3)$$

where μ is the viscosity, I is the unit tensor.

Total enthalpy form of the energy equation

$$\frac{\partial}{\partial t}(\rho H) + \nabla \cdot (\rho \vec{v} H) = \nabla \cdot \left(\frac{k_t}{c_p} \nabla H \right) + S_h, \quad (4)$$

where k_t is the turbulent thermal conductivity, defined according to the turbulence model being used). S_h includes the heat of chemical reaction and any other volumetric heat sources.

Conservation equations for chemical species

$$\frac{\partial}{\partial t}(\rho Y_i) + \nabla \cdot (\rho \vec{v} Y_i) = -\nabla \cdot \vec{J}_i + R_i, \quad (5)$$

where Y_i is the local mass fraction of each species and \vec{J}_j is the diffusion flux of species j .

$$\vec{J}_i = -\rho D_{i,m} \nabla Y_i - D_{T,i} \frac{\nabla T}{T}. \quad (6)$$

Chemical mechanisms for combustion often involve multiple reactions and multiple species [22]. Consider a multistep chemical mechanism with n_s species reacting through n_r number of chemical reactions. The chemical reaction rate, R_i , which is primarily a function of the concentration and temperature of the contributing species is expressed by the following equation:

$$R_i = W_I \sum_{J=1}^{n_r} (\nu''_{I,J} - \nu'_{I,J}) \left(k_J^{(f)} \prod_{I=1}^{n_s} \left(\frac{X_{IP}}{R_u T} \right)^{\nu'_{I,J}} - k_J^{(r)} \prod_{I=1}^{n_s} \left(\frac{X_{IP}}{R_u T} \right)^{\nu''_{I,J}} \right). \quad (7)$$

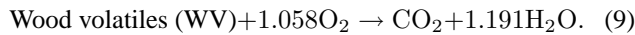
Here, W_I is the molecular weight for I -th chemical species, while $\nu'_{I,J}$ and $\nu''_{I,J}$ are the stoichiometric coefficients for the reactant and product side of the elementary reaction, respectively. $k_J^{(f)}$ and $k_J^{(r)}$ are the forward and reverse reaction rate constants for the J -th reaction in a multistep chemical mechanism, respectively. The mole fraction of I -th species is X_I . The Arrhenius rate laws are used for the elementary reaction rate constant:

$$k_J^{(f)}(T) = A_J^{(f)} T^{b_J} \exp\left(-\frac{E_{a,J}^{(f)}}{R_u T}\right). \quad (8)$$

Here, $A_J^{(f)}$ is the pre-exponential factor, b_J is the temperature exponent and $E_{a,J}^{(f)}$ is the activation energy.

2.2. Numerical methodology

Governing equations were solved with ANSYS FluentTM using a pressure-based formulation considering buoyant effects and a mixture of wood volatiles and air. User-defined functions were used for temperature-dependent properties of the mixture of wood volatiles and air (O_2 , CO_2 , H_2O and N_2). Nitrogen is treated as inert and the other species are linked through a single irreversible finite-rate chemical reaction [23]:



The density was modeled with the ideal gas law. Piecewise approximations for specific heat and thermal conductivity were considered, whereas for the viscosity, the Sutherland model was used. In our calculations, the energy released by wood combustion is replaced by wood volatiles released from a surface in the combustion region, see Núñez *et al.* [24] for a detailed explanation.

The realizable $\kappa - \epsilon$ model was implemented with enhancement wall treatment for pressure and thermal effects. The species equations consider a volumetric reaction with a stiff chemistry solver, whereas turbulence chemistry is neglected. The SIMPLEC method is used with body weighted pressure and second-order upwind for the velocity and species. Continuity convergence criteria is set to 1e-06.

2.2.1. Boundary conditions

In modeling biomass stoves specification of boundary conditions is critical for obtaining realistic simulation results that reflect real-world operating conditions because there are no predefined conditions.

To estimate the inlet mass flow rate, an excess oxygen ratio of 2 can be considered to ensure a sufficient mixing O_2 /wood volatiles [25]. When mass flow boundary conditions are used for an inlet zone, a velocity is computed for each face in that zone:

$$\rho v_n = \frac{\dot{m}}{A}. \quad (10)$$

Pressure inlet boundary conditions can be used when the inlet pressure is known but the flow rate and/or velocity is not known. This situation may arise in many practical situations, including buoyancy-driven flows. The pressure field (including all pressure inputs) will include the hydrostatic head. In incompressible flow, the inlet total pressure and the static pressure, p_s , are related to the inlet velocity via Bernoulli's equation:

$$p_0 = p_s + \frac{1}{2}\rho v^2. \quad (11)$$

For the upper surface of the comal, a convective heat transfer coefficient of 38.9 W/m²K reported by [26] is used. This value was obtained from experiments on a plancha-type cookstove. For the external walls of the chimney, a convective coefficient of 15 W/m²K is fixed [7], and the conduction resistance of a thin layer of steel is taken into account.

The ambient temperature was fixed to 298 K. At the outlet zone, the mole fraction of CO_2 was 46 % according to the stoichiometric calculations. For the rest of the walls (identified as wall zone) an adiabatic condition was assumed since an insulation fiber (Thermal ceramic) was used to cover the inner parts of the stove.

Heat transfer processes (conduction, convection, and radiation) are important phenomena in cookstoves. In our simulations, the conduction phenomenon takes place on the comal (solid) domain; whereas convection occurs due to the buoyancy force, and in the convective cooling of the surfaces of the cookstove (boundary conditions).

3. Results and discussion

3.1. CAD design and forced convection test

The griddle is a critical component of the stove, serving as the primary area for effective heat delivery. To assess its influence on heat transfer, parameterization techniques were employed, facilitating the execution of seven virtual experiments on CAD models derived from the design of the stove. This approach enables a detailed analysis of how the geometry of the griddle impacts the heat distribution. The visual representation of these models is detailed in Fig. 2. Table I

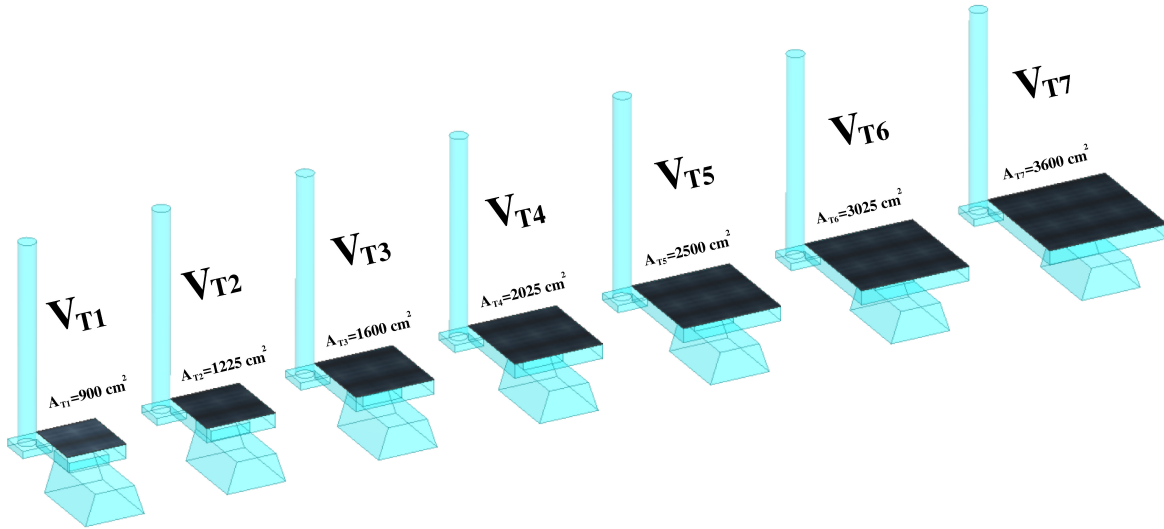


FIGURE 2. Parametric internal volume generation. Griddle area $25 \times 25 \text{ cm}^2$ - $60 \times 60 \text{ cm}^2$.

TABLE I. Properties of different griddle sizes.

Case	Area cm^2	Cells	Aspect ratio	Orthogonality
V_{T1}	25×25	644,772	3.057	0.988
V_{T2}	30×30	667,722	3.733	0.989
V_{T3}	35×35	710,674	4.042	0.990
V_{T4}	40×40	791,922	4.171	0.989
V_{T5}	45×45	834,773	4.492	0.990
V_{T6}	50×50	876,870	4.807	0.991
V_{T7}	55×55	897,328	5.233	0.991

TABLE II. Mesh size, time t_s , temperature T_{ca} , and number of cells.

Mesh size	t_s [h]	T_{ca} [K]	Cells
Extra-coarse (M_{ec})	0.7503	374.8215	251 005
Coarse (M_{co})	1.5759	374.9220	432 003
Medium (M_{me})	2.2558	374.8341	644 772
Fine (M_{fi})	3.6110	374.9593	962 862
Extra-fine (M_{ef})	6.2307	374.6582	1 567 665

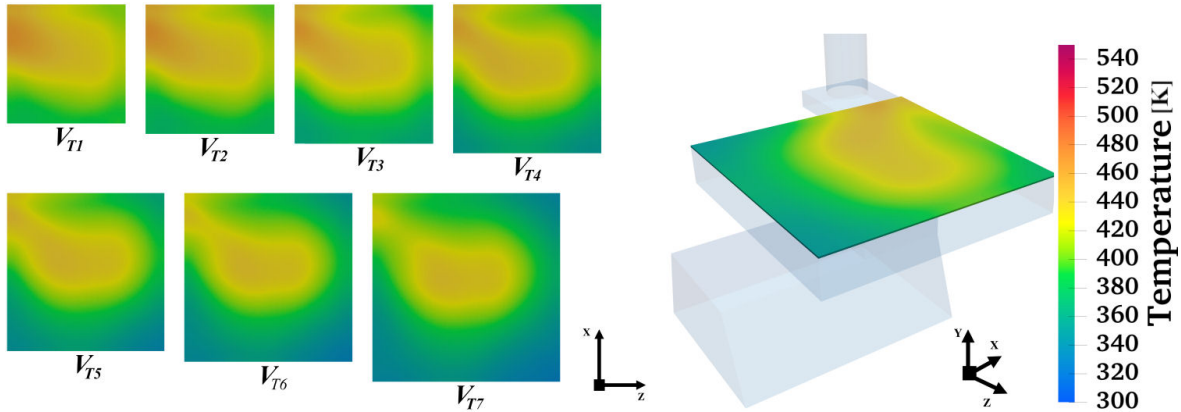


FIGURE 3. Temperature distribution on the griddle.

provides the characteristics of each design, namely the griddle area and the number of computational cells utilized in the simulations. Table II provides a sensitivity analyses and computational times. The medium mesh provides good accuracy with few computational times through the use of hexahedral cells.

The analysis provides sensitivity analyses and computational times. The medium mesh provides good accuracy with few computational times through the use of hexahedral cells.

Hexahedral meshes were used with a zone refinement, following the meshing methodology reported by Gómez-Heleria [27]. This approach maintained a consistent flow and temperature to ensure an output power of 7.26 kW under steady-state. The resulting temperature distribution across the griddle is depicted in Fig. 3, including the maximum and minimum temperatures achieved.

The results indicate that the temperature is higher in the upper right corner direction because the air is injected from

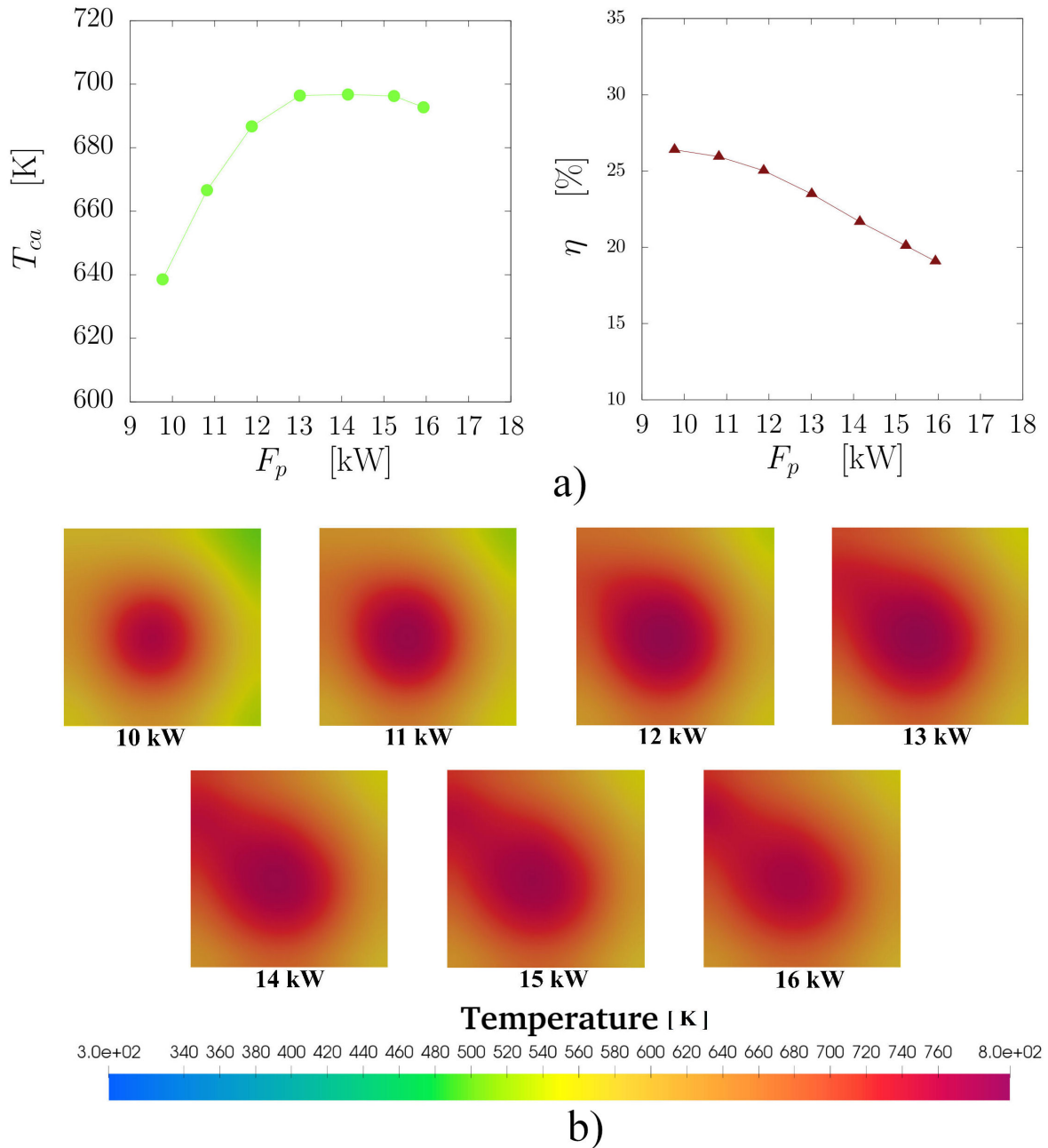


FIGURE 4. Temperature over the comal and the thermal efficiency as a function of the firepower.

the combustion chamber entrance. This virtual prototype development process serves as a basis for decision-making, in order to modify the geometry or adjust operating conditions.

In addition to thermal performance, other factors should be considered when determining the selected interior volume for the stove design. The temperature in the griddle should have an adequate range for the cooking task, generally making tortillas. The griddle area should be adjusted to a production capacity; the users suggest 4 pieces in this case. Also, the griddle area should correspond to standard market dimensions. After considering all of these factors, it was determined that the VT5 geometry produced satisfactory results.

3.2. Combustion modeling

The selected inner volume was used to calculate heat transfer, considering combustion reactions. Calculations were performed for different firepower values in a range of 10-16 kW. Figure 4 shows the temperature field that is reached in the comal. Note that the temperature distribution crosses the diagonal part of the griddle.

The intentionally planned diagonal temperature distribution serves a functional purpose, aligning with the practical needs of users. The quadrant closest to the chimney, being the hottest zone, is optimally suited for pots and pans that require higher temperatures for cooking. Conversely, the

cooler quadrants are ideally utilized for tasks such as making tortillas, which necessitate lower heat. This strategic layout ensures that the griddle accommodates diverse cooking activities simultaneously, maximizing efficiency and user convenience.

The CO_2 and H_2O distribution affects the efficiency of combustion processes. Incomplete combustion leads to the production of carbon monoxide (CO) and unburned hydrocarbons, which is less desirable from both an efficiency and emissions standpoint.

Finally, the average temperature over the comal and the thermal efficiency are evaluated as a function of the firepower (see Fig. 4).

It can be seen that it reaches a temperature of around 700 K, and the temperature also decreases at a large firepower value. It can be related to a reduction in the thermal efficiency at large firepower due to the increase of convective losses at the griddle.

3.3. From design to a prototype

A design with all of the functionalities of the stove was created using the insights gained from CFD simulations for the thermal performance of the control volume and the constraints imposed by the requirements of the user. The cookstove is created by fabricating the interior volume in sheet metal and adding a casing that provides support and additional functionality, as shown in Fig. 5.

An initial 3D-printed prototype was fabricated from the CAD designs [27]. It was an instrumental tool for introducing the initial concept to users, allowing them to become involved with the design and providing a tangible representation of the stove. Furthermore, this preliminary model played a crucial role in assessing the usability of the device. The prototype

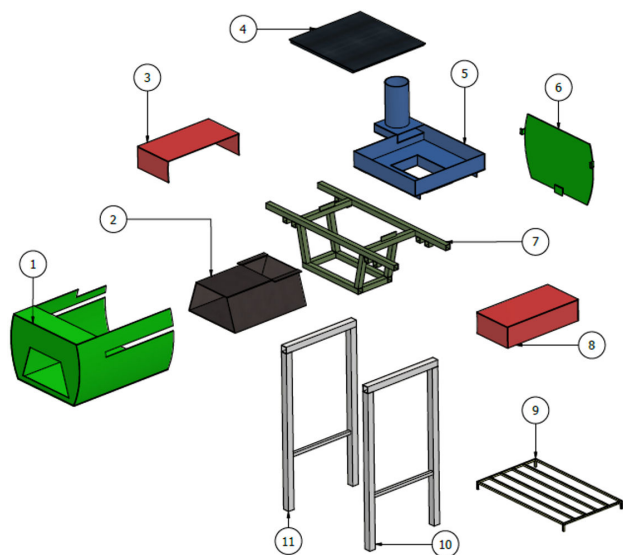


FIGURE 5. Sheet metal components. 1) Casing, 2) combustion chamber, 3) right eaves, 4) comal, 5) lateral cross-flow structure, 6) rear door, 7) structural support 8) left eaves, 9) firewood storage support, 10) and 11) Legs [27].

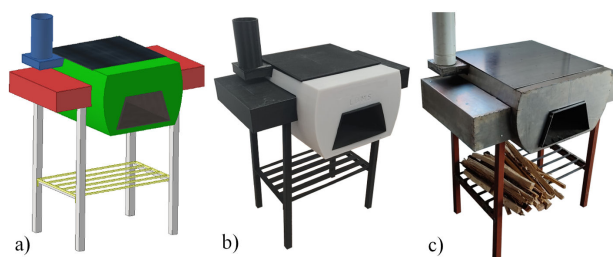


FIGURE 6. a) CAD design, b) prototype, c) manufactured stove [27].

was also printed to ensure that all parts fit together correctly and that there were no obstructions that could interfere with the stove's functionality. This phase was essential in validating the design born from CFD analyses before proceeding to the construction of the final sheet metal version, depicted in Fig. 6c).

3.4. Experimental test

The experimental validation of the model is discussed in the following Refs. [25,28-30], which were developed by our research team. These references provide in-depth information on the experimental results and validation processes.

Governments, international organizations, and non-governmental organizations (NGOs) often establish performance standards and certification programs for biomass stoves to ensure they meet certain criteria related to emissions, efficiency, and safety. Emission and water boiling tests (WBT) are typically part of the certification process. This protocol only evaluates global parameters such as the thermal efficiency of the stove [31,32]. The result of the test is presented in Table III.

The thermal efficiency from CFD results is compared with experimental data from WBT. The average firepower is 16 kW and the thermal efficiency is 15% as can be seen in Table III. The numerical solution achieves a thermal efficiency around 18%.

A field evaluation of the stove was carried out in a rural setting, enabling users to participate in practical cooking tests. This hands-on assessment proved vital in gauging the initial of the stove acceptance, particularly through user interaction and operational testing (See Fig. 7).

TABLE III. WBT tests on cold comal (CS) and hot comal (HS) after modifications.

Calculations/Results	Units	WBT A		WBT B	
		CS	HS	CS	HS
Time to boil Pot #1	min	23	17	21	17
Thermal efficiency	%	13	15	14	16
Burning rate	g/min	49	56	51	57
Firepower	kW	14	16	14.8	16.5



FIGURE 7. a) Evaluation of the users, b) final prototype.

By incorporating feedback from real-world stove operations, design can be continuously improved to achieve greater efficiency, quality, and sustainability, ensuring greater adoption and benefits. Following the field evaluation, several modifications were implemented to improve the performance of the stove and safety. In particular, the insulation was improved, serving a dual purpose: it reduces energy loss and improves safety by protecting users from high surface temperatures (see Table III).

4. Conclusions

Numerical simulation of fluid dynamics allowed the elaboration of a prototype of a stove. Heat transfer, fluid flow, and combustion were evaluated. It is possible to develop more complex models for combustion phenomena, but the development of rapid prototypes is crucial to know the user experience. Key findings reveal a strategic diagonal temperature

distribution across the comal, significantly enhancing cooking versatility and energy utilization. Furthermore, modifications such as enhanced insulation and reduced start-up times have increased the stove's thermal efficiency and user experience.

The development of our stove model integrated advanced design, rigorous testing, and user feedback to ensure both efficiency and user satisfaction. The significance of this study lies in its methodological approach, which bridges the gap between theoretical models and real-world usability. The findings contribute to a deeper understanding of how stove design can be tailored to meet both efficiency standards and user expectations, thus improving the adoption of cleaner cooking solutions in underserved communities. The methodology encompassed the utilization of Computer-Aided Design (CAD), the creation of 3D-printed prototypes, and the subsequent manufacturing of a metal stove. The presented methodology is versatile and can be applied to the production of various stove prototypes and it is important to note that the interior volume is the heart of the stove, since it is where the physical phenomena occur.

This stove model prioritizes adoption based on feedback from user interactions in rural communities. In this case, the progression from CFD to diffusion and adoption in rural communities is investigated. By directly engaging with users and incorporating their feedback, the design process is more likely to be accepted because the stove is not only technically efficient, but also culturally and practically appropriate for the community's needs.

Future research should expand upon this work by exploring a wider range of stove designs, materials, and user environments. Investigating the long-term durability of stove modifications and their impact on emissions over time would provide valuable insights for developing universally applicable, sustainable cooking solutions.

Acknowledgments

Authors would like to acknowledge project CONAHCyT-PRONACES 319333. Yovany Galindo would like to thank CONAHCYT for a postdoctoral fellowship. This work was supported by UNAM Posdoctoral Program (POSDOC). D. Gómez-Heleria would like to thank DGAPA-UNAM for a postdoctoral fellowship. Authors also acknowledge Dr. Víctor M. Ruiz-García and MSc. Juan C. Vázquez-Tinoco from IIES-UNAM for their support in the experimental tests. CFD computations and experimental measurements were performed at the Laboratory for Design, Modeling and Simulations (LDMS) at the Morelia Unit of the IIM-UNAM and at the Laboratory for Innovation and Evaluation in Bioenergy (LINEB) at IIES-UNAM, respectively. We would like to thank the San Francisco Pichátaro community for their valuable contributions to our research.

1. S. A. Mehetre *et al.*, Improved biomass cookstoves for sustainable development: A review, *Renewable and Sustainable Energy Reviews* **73** (2017) 672, <https://doi.org/10.1016/j.rser.2017.01.150>.
2. L. A. de la Sierra-de la Vega *et al.*, Implementation process evaluation of an improved cookstove program in rural San Luis Potosi, Mexico, *Energy for Sustainable Development* **66** (2022) 44, <https://doi.org/10.1016/j.esd.2021.11.003>.
3. S. S. Ghiwe, V. R. Kalamkar, and P. D. Sawarkar, Performance Optimization of Hybrid Draft Biomass Cookstove Using CFD, *Combustion Science and Technology* (2023) 1, <https://doi.org/10.1080/00102202.2023.2221817>.
4. P. Medina *et al.*, Comparative performance of five Mexican plancha-type cookstoves using water boiling tests, *Development Engineering* **2** (2017) 20, <https://doi.org/10.1016/j.deveng.2016.06.001>.
5. E. Adkins *et al.*, Field testing and survey evaluation of household biomass cookstoves in rural sub-Saharan Africa, *Energy for Sustainable Development* **14** (2010) 172, <https://doi.org/10.1016/j.esd.2010.07.003>.
6. M. Sedighi and H. Salarian, A comprehensive review of technical aspects of biomass cookstoves, *Renewable and Sustainable Energy Reviews* **70** (2017) 656, <https://doi.org/10.1016/j.rser.2016.11.175>.
7. N. A. MacCarty and K. M. Bryden, A generalized heat-transfer model for shielded-fire household cookstoves, *Energy for Sustainable Development* **33** (2016) 96, <https://doi.org/10.1016/j.esd.2016.03.003>.
8. J. Prapas *et al.*, Influence of chimneys on combustion characteristics of buoyantly driven biomass stoves, *Energy for Sustainable Development* **23** (2014) 286, <https://doi.org/10.1016/j.esd.2014.08.007>.
9. P. Medina, A. Mora, and A. Beltrán, Combustion efficiency and CO/NO_x emissions for a biomass plancha-type stove: Effect of the air excess ratio, *Thermal Science and Engineering Progress* **48** (2024) 102411, <https://doi.org/10.1016/j.tsep.2024.102411>.
10. J. J. Caubel *et al.*, Optimization of Secondary Air Injection in a Wood-Burning Cookstove: An Experimental Study, *Environmental Science & Technology* **52** (2018) 4449, <https://doi.org/10.1021/acs.est.7b05277>.
11. M. Koraiem and D. Assanis, Wood stove combustion modeling and simulation: Technical review and recommendations, *International Communications in Heat and Mass Transfer* **127** (2021) 105423, <https://doi.org/10.1016/j.icheatmasstransfer.2021.105423>.
12. R. Scharler *et al.*, Transient CFD simulation of wood log combustion in stoves, *Renewable Energy* **145** (2020) 651, <https://doi.org/10.1016/j.renene.2019.06.053>.
13. L. Borraz *et al.*, Transient CFD simulations of a biomass plancha-type cookstove using free software, *Journal of the Brazilian Society of Mechanical Sciences and Engineering* **44** (2022) 340, <https://doi.org/10.1007/s40430-022-03654-0>.
14. S. O'Shaughnessy *et al.*, Adaptive design of a prototype electricity-producing biomass cooking stove, *Energy for Sustainable Development* **28** (2015) 41, <https://doi.org/10.1016/j.esd.2015.06.005>.
15. B. Y. Mekonnen, Computational study of a novel combined cookstove for developing countries, *African Journal of Science, Technology, Innovation and Development* **13** (2021) 657, <https://doi.org/10.1080/20421338.2020.1865511>.
16. J. Phusrimuang and T. Wongwuttanasatian, Improvements on thermal efficiency of a biomass stove for a steaming process in Thailand, *Applied Thermal Engineering* **98** (2016) 196, <https://doi.org/10.1016/j.applthermaleng.2015.10.022>.
17. K. S. Thacker, K. M. Barger, and C. A. Mattson, Balancing technical and user objectives in the redesign of a peruvian cookstove, *Development Engineering* **2** (2017) 12, <https://doi.org/10.1016/j.deveng.2016.05.001>.
18. S. Dalbehera, S. S. Ghiwe, and V. R. Kalamkar, Numerical analysis of design modifications in a natural draft biomass rocket cookstove, *Sustainable Energy Technologies and Assessments* **54** (2022) 102858, <https://doi.org/10.1016/j.seta.2022.102858>.
19. P. Motyl, *et al.*, A New Design for Wood Stoves Based on Numerical Analysis and Experimental Research, *Energies* **13** (2020) 1028, <https://doi.org/10.3390/en13051028>.
20. A. Fluent, ANSYS fluent theory guide 15.0, ANSYS, Canonsburg, PA **33** (2013)
21. T. Poinsoot and D. Veynante, Theoretical and Numerical Combustion (R.T. Edwards, Inc., 2005).
22. S. De *et al.*, eds., Modeling and Simulation of Turbulent Combustion, Energy, Environment, and Sustainability (Springer Berlin Heidelberg, New York, NY, 2018).
23. S. S. Ghiwe *et al.*, Numerical and experimental study on the performance of a hybrid draft biomass cookstove, *Renewable Energy* **205** (2023) 53, <https://doi.org/10.1016/j.renene.2023.01.077>.
24. J. Núñez *et al.*, Natural-draft flow and heat transfer in a plancha-type biomass cookstove, *Renewable Energy* **146** (2020) 727, <https://doi.org/10.1016/j.renene.2019.07.007>.
25. P. Medina *et al.*, Experimental and numerical comparison of CO₂ mass flow rate emissions, combustion and thermal performance for a biomass plancha-type cookstove, *Energy for Sustainable Development* **63** (2021) 153, <https://doi.org/10.1016/j.esd.2021.07.001>.
26. J. Prapas, Toward the understanding and optimization of chimneys for buoyantly driven biomass stoves, Ph.D. thesis, Colorado State University (2013).
27. D. Gómez-Heleria, Modelado y Simulación de Fenómenos de Transporte en Estufas de Biomasa, Ph.D. thesis, Universidad Nacional Autónoma de México (2023).

28. J. Núñez *et al.*, Natural-draft flow and heat transfer in a plancha-type biomass cookstove, *Renewable Energy* **146** (2020) 727, <https://doi.org/10.1016/j.renene.2019.07.007>.
29. D. Gómez-Helería *et al.*, Steady-state behavior of a biomass plancha-type cookstove: Experimental and 3D numerical study, *Sustainable Energy Technologies and Assessments* **57** (2023) 103172, <https://doi.org/10.1016/j.seta.2023.103172>.
30. P. Medina *et al.*, Transport phenomena in a biomass planchatype cookstove: Experimental performance and numerical simulations, *Energy for Sustainable Development* **71** (2022) 132, <https://doi.org/10.1016/j.esd.2022.09.019>.
31. C. C. Alliance *et al.*, The water boiling test, version 4.2. 3: Cookstove emissions and efficiency in a controlled laboratory setting, Glob. Alliances Clear. *Cookstoves* **2** (2013) 52
32. J. Jetter *et al.*, Pollutant Emissions and Energy Efficiency under Controlled Conditions for Household Biomass Cookstoves and Implications for Metrics Useful in Setting International Test Standards, *Environmental Science & Technology* **46** (2012) 10827, <https://doi.org/10.1021/es301693f>.
33. H. Zhou *et al.*, Combustion temperature in a threedimensional porous stove with a high-fidelity structure, *Applied Thermal Engineering* **233** (2023) 121108, <https://doi.org/10.1016/j.applthermaleng.2023.121108>.
34. S. R. Kashyap, S. Pramanik, and R. Ravikrishna, A review of energy-efficient domestic cookstoves, *Applied Thermal Engineering* **236** (2024) 121510, <https://doi.org/10.1016/j.applthermaleng.2023.121510>.
35. M. K. Commeh *et al.*, CFD analysis of a flat bottom institutional cookstove, *Scientific African* **16** (2022) e01117, <https://doi.org/10.1016/j.sciaf.2022.e01117>.
36. R. R. Pande, V. R. Kalamkar, and M. P. Kshirsagar, The Effect of Inlet Area Ratio on the Performance of Multipot Natural Draft Biomass Cookstove, Proceedings of the National Academy of Sciences, *India Section A: Physical Sciences* **92** (2022) 479, <https://doi.org/10.1007/s40010-019-00650-3>.
37. M. Barbour *et al.*, Development of wood-burning rocket cookstove with forced air-injection, *Energy for Sustainable Development* **65** (2021) 12, <https://doi.org/10.1016/j.esd.2021.09.003>.
38. K. B. Sutar *et al.*, Biomass cookstoves: A review of technical aspects, *Renewable and Sustainable Energy Reviews* **41** (2015) 1128, <https://doi.org/10.1016/j.rser.2014.09.003>.